NeuroImage 149 (2017) 85–97

Contents lists available at ScienceDirect

NeuroImage

journal homepage: www.elsevier.com/locate/neuroimage

Disentangling resting-state BOLD variability and PCC functional connectivity in 22q11.2 deletion syndrome

Daniela Zöller[a,b,c,*], Marie Schaer[c], Elisa Scariati[c], Maria Carmela Padula[c], Stephan Eliez[c], Dimitri Van De Ville[a,b]

[a] Medical Image Processing Laboratory, Institute of Bioengineering, École Polytechnique Fédérale de Lausanne (EPFL), Lausanne, Switzerland
[b] Department of Radiology and Medical Informatics, University of Geneva, Geneva, Switzerland
[c] Developmental Imaging and Psychopathology Laboratory, Office Médico-Pédagogique, Department of Psychiatry, University of Geneva, Geneva, Switzerland

ARTICLE INFO

Keywords:
Resting-state fMRI
BOLD signal variability
Functional connectivity
Default mode network
22q11.2 deletion syndrome

ABSTRACT

Although often ignored in fMRI studies, moment-to-moment variability of blood oxygenation level dependent (BOLD) signals reveals important information about brain function. Indeed, higher brain signal variability has been associated with better cognitive performance in young adults compared to children and elderly adults. Functional connectivity, a very common approach in resting-state fMRI analysis, is scaled for variance. Thus, alterations might be confounded or driven by BOLD signal variance alterations. Chromosome 22q11.2 deletion syndrome (22q11.2DS) is a neurodevelopmental disorder that is associated with a vast cognitive and clinical phenotype. To date, several resting-state fMRI studies reported altered functional connectivity in 22q11.2DS, however BOLD signal variance has not yet been analyzed. Here, we employed PLS correlation analysis to reveal multivariate patterns of diagnosis-related alterations and age-relationship throughout the cortex of 50 patients between 9 and 25 years old and 50 healthy controls in the same age range. To address how functional connectivity in the default mode network is influenced by BOLD signal fluctuations, we conducted the same analysis on seed-to-voxel connectivity of the posterior cingulate cortex (PCC) and compared resulting brain patterns. BOLD signal variance was lower mainly in regions of the default mode network and in the dorsolateral prefrontal cortex, but higher in large parts of the temporal lobes. In those regions, BOLD signal variance was correlated with age in healthy controls, but not in patients, suggesting deviant developmental trajectories from child- to adulthood. Positive connectivity of the PCC within the default mode network as well as negative connectivity towards the frontoparietal network were weaker in patients with 22q11.2DS. We furthermore showed that lower functional connectivity of the PCC was not driven by higher BOLD signal variability. Our results confirm the strong implication of BOLD variance in aging and give an initial insight in its relationship with functional connectivity in the DMN.

1. Introduction

Inter- and intra-subject variability of resting-state functional magnetic resonance imaging (rs-fMRI), such as between-trial variability (Poldrack et al., 2015; Laumann et al., 2015; Davis et al., 2014), spatial variability between voxels (Davis et al., 2014; Gopal et al., 2016) and moment-to-moment variability of blood oxygenation level dependent (BOLD) signals within every voxel (McIntosh et al., 2010; Deco et al., 2011; Allen et al., 2014) have gained interest in recent literature. Such variability measures are rarely taken into account in conventional rs-fMRI analysis, but their consideration might give a deeper insight into underlying brain processes and their connection to disease-related alterations (McIntosh et al., 2010; Gopal et al., 2016). Even though the exact implications of the latter, moment-to-moment BOLD signal variability, are not clear yet, theoretical work has suggested that spontaneous signal fluctuations are crucial for neural system functions

Abbreviation: 22q11.2DS, chromosome 22q11.2 deletion syndrome; ALFF, amplitude of low-frequency fluctuations; BOLD, blood oxygenation level dependent; DARTEL, Diffeomorphic Anatomical Registration using Exponentiated Lie algebra; DMN, default mode network; DPARSF, Data Processing Assistant for Resting-State fMRI; EEG, electroencephalography; fMRI, functional magnetic resonance imaging; FWHM, full width half maximum; HC, healthy control; IBASPM, Individual Brain Atlases using Statistical Parametric Mapping; LV, latent variable; MEG, magnetoencephalography; PCC, posterior cingulate cortex; PLS, partial least squares; rs-fMRI, resting-state functional magnetic resonance imaging; RSN, resting-state network; SD_{BOLD}, BOLD signal standard deviation; SVD, singular value decomposition

* Corresponding author at: Department of Radiology and Medical Informatics, University of Geneva, Geneva, Switzerland.
E-mail address: daniela.zoller@epfl.ch (D. Zöller).

http://dx.doi.org/10.1016/j.neuroimage.2017.01.064
Received 7 July 2016; Accepted 26 January 2017
Available online 29 January 2017
1053-8119/

and reflect larger network complexity and dynamic range (Deco et al., 2011; McIntosh et al., 2010). Several studies focusing on the implications of BOLD signal variability on aging and cognitive performance in adults have demonstrated that moment-to-moment variability is not just noise as previously assumed, but is higher in better performing, younger adults compared to lower performing, elderly subjects (Garrett et al., 2013a, 2014; Grady and Garrett, 2014). Findings in other modalities such as EEG (McIntosh et al., 2008; Lippé et al., 2009) and MEG (Misić et al., 2010) support those findings, suggesting lower brain variability in children compared to young adults. Moment-to-moment BOLD signal fluctuations have been shown to be altered in multiple neuropsychiatric disorders such as autism (Di Martino et al., 2014; Lai et al., 2010), Alzheimer's disease (Zhao et al., 2014; Liu et al., 2014; Han et al., 2011; Xi et al., 2012) and attention deficit hyperactivity disorder (Zang et al., 2007), as well as schizophrenia (Yu et al., 2014; Yang et al., 2014; Liu et al., 2016). The strong relationship of BOLD signal variability with age and cognitive performance make this approach especially promising to obtain further insight in the mechanisms driving the development of cognitive and psychiatric disorders.

Rs-fMRI has been widely used in recent years to analyze altered brain function in numerous psychiatric diseases. It is especially advantageous when studying populations with limited abilities to respond to task, such as young children or individuals with impaired cognitive functions and attention deficits. Most rs-fMRI studies focus on stationary functional connectivity, assessed by computing the temporal correlation between the BOLD signals of different brain regions computed over the whole resting-state session. However, conventional functional connectivity is normalized for BOLD signal variance. In other words, the Pearson correlation coefficient is scaled with respect to individual signal standard deviation and BOLD signal variability might even confound results of functional connectivity (Garrett et al., 2013b). For instance, lower functional connectivity might result from higher variance, or oppositely, lower variance might have weakened the effect of functional connectivity reduction.

Chromosome 22q11.2 deletion syndrome (22q11.2DS) is a neurodevelopmental disorder caused by a microdeletion in chromosome 22. It occurs in approximately 1 out of 4000 live births and comes with a vast phenotype that includes somatic, cognitive and psychiatric features (Oskarsdóttir et al., 2004). Amongst others, patients with 22q11.2DS suffer from a wide range of cognitive impairments, including mild mental delay and impaired executive functions (Maeder et al., 2016; Antshel et al., 2008; Niklasson and Gillberg, 2010; Swillen et al., 1997). Furthermore, 22q11.2DS comes with a very high risk of developing schizophrenia, which occurs in 30% to 40% of patients (Lewandowski et al., 2007; Murphy et al., 1999; Schneider et al., 2014). The developmental characteristics of the disease and the high risk of psychotic symptoms makes 22q11.2DS a unique model for the study of behavioral, clinical and neural markers in schizophrenia in order to improve treatments and prevention (Bassett and Chow, 1999).

In 22q11.2DS, to date, several studies have analyzed functional connectivity during rest (Debbané et al., 2012; Padula et al., 2015; Scariati et al., 2014; Schreiner et al., 2014; Mattiaccio et al., 2016). They have revealed altered connectivity in multiple resting-state networks (RSNs) such as the visuospatial, sensory-motor and default mode networks. Two of the studies (Padula et al., 2015; Schreiner et al., 2014) specifically focused on connectivity of the default mode network (DMN), a RSN that has been associated with self-referential, autobiographical mental processes and social cognition (Greicius et al., 2003; Fair et al., 2008; Qin and Northoff, 2011). They revealed decreased connectivity in 22q11.2DS, especially between anterior-posterior regions (Schreiner et al., 2014; Padula et al., 2015). Alterations within the DMN have furthermore been associated with dysfunctional social behavior (Schreiner et al., 2014) as well as psychotic symptoms (Debbané et al., 2012; Mattiaccio et al., 2016).

To our best knowledge, no studies to date have investigated BOLD signal variability in 22q11.2DS. Given its link to development and cognition, we hypothesize that BOLD signal variability is broadly altered in 22q11.2DS and that it is increasing during development from child- to adulthood. We used the BOLD signal standard deviation (SD_{BOLD}) to measure brain variability. We then employed multivariate partial least squares (PLS) correlation (Krishnan et al., 2011; McIntosh et al., 2004) in order to identify multivariate brain variability alterations and developmental characteristics in our 22q11.2DS cohort compared to controls. PLS correlation is better suited for voxelwise brain analysis than mass-univariate approaches, as they assume independence between all voxels (a hypothesis which is obviously wrong in the brain) and are thus very limited by the problem of multiple comparisons. PLS correlation measures multivariate relationship between two sets of variables (here: voxelwise SD_{BOLD} on one side and a combination of subject-specific design variables, i.e. diagnosis, age and age by diagnosis interaction, on the other side). Its second advantage in addition to multivariability of the brain pattern is thus the possibility to investigate the relationship of brain data with multiple external variables at the same time. We secondly hypothesize that conventional functional connectivity analysis might be influenced by BOLD variation, as Pearson correlation is normalized for standard deviation. To obtain an insight on possible links between functional connectivity and brain variability, we selected a seed inside the posterior cingulate cortex (PCC) and analyzed brain-wide seed-to-voxel connectivity. The PCC was selected as it is a central hub inside the DMN, one of the best studied RSN (Greicius et al., 2003; Fair et al., 2008; Menon and Uddin, 2010). It additionally appeared as a region of strongly decreased SD_{BOLD} variability during the first analysis. We used the same PLS approach as before to identify multivariate alterations and age-relationship of PCC functional connectivity. In a last step we identified regions where both functional connectivity and BOLD signal variance were altered in our cohort. In those regions, SD_{BOLD} might confound or even drive functional connectivity alterations. Thus, we compared the direction of alteration of both measures in those regions, in order to obtain a first insight in the relationship between BOLD variability and functional connectivity.

2. Methods

2.1. Participants

Fifty patients with 22q11.2DS aged between 9 and 25 (M/F=21/29, mean age=16.53 ± 4.25 years) were included in the study (see Table 1). The control group comprised fifty healthy subjects in the same age range (M/F=22/28, mean age=16.44 ± 4.20 years). Healthy controls (HCs) were recruited amongst siblings of our patients and through the Geneva state school system.

From our initial sample of 110 patients and 75 HCs between 9 and 25 years old, a total of 85 participants had to be excluded to ensure the good quality of the data. Five subjects (only patients) were excluded because they reported having fallen asleep during the scanning session. Another 34 subjects (5 HC) had to be excluded due to excessive motion of more than 3 mm in translation or 3° in rotation and the data of 35 more subjects (19 HC) were not used because parts of the cortex were not captured. From the remaining dataset, 11 more participants (1 HC) were excluded after motion scrubbing (Power et al., 2012, see paragraph *Preprocessing*) as less than 100 rs-fMRI scans, corresponding to 4 min of scanning time, had a framewise displacement below the threshold of 0.5 mm. Table 2 shows a summary of motion data within the two groups.

Written informed consent was received from participants and their parents (for subjects younger than 18 years old). The research protocols were approved by the Institutional Review Board of Geneva University School of Medicine. The cohort is partly overlapping with our previous rs-fMRI studies: 33 subjects (15 HC) have been also included in Debbané et al. (2012), 52 subjects (27 HC) in Scariati et al.

Table 1
Demographic information.

	HC	22q11.2DS	p value
Number of subjects (M/F)	50 (22/28)	50 (21/29)	0.910
Age mean ± SD (range)	16.44 ± 4.20 (9.5-24.9)	16.53 ± 4.25 (9.0-24.8)	0.840
Right handed*	71.43%	80.95%	
IQ**	109.68 ± 12.99	68.20 ± 12.21	<0.001
N. subjects meeting criteria for psychiatric diagnosis	**N/A**	**27 (54%)**	
Anxiety disorder	N/A	8	
Attention deficit hyperactivity disorder	N/A	2	
Mood disorder	N/A	4	
Schizophrenia	N/A	1	
More than one psychiatric disorder	N/A	12	
N. subjects medicated	**0**	**14**	
Methylphenidate	0	8	
Antipsychotics	0	2	
Anticonvulsants	0	1	
More than one class of medication	0	3	

* Handedness was measured using the Edinburgh laterality quotient, right handedness was defined by a score of more than 50.
** IQ was measured using the Wechsler Intelligence Scale for Children–III (Wechsler, 1991) for children and the Wechsler Adult Intelligence Scale–III (Wechsler, 1997) for adults.

Table 2
fMRI motion parameters. FD - framewise displacement.

		HC	22q11.2DS	p value	correlation with age (p value)
Mean translation (mm)	x	0.13 ± 0.13	0.12 ± 0.14	0.7411	0.04 (0.6851)
	y	0.19 ± 0.14	0.18 ± 0.18	0.8446	0.03 (0.7994)
	z	0.31 ± 0.29	0.39 ± 0.34	0.1670	−0.10 (0.3222)
Mean rotation (degree)	r_x	0.34 ± 0.27	0.39 ± 0.30	0.3149	−0.04 (0.7260)
	r_y	0.20 ± 0.17	0.18 ± 0.14	0.6221	−0.14 (0.1661)
	r_z	0.17 ± 0.17	0.19 ± 0.19	0.5786	−0.05 (0.6430)
Mean FD (mm), before scrubbing		0.16 ± 0.10	0.22 ± 0.11	<0.001	−0.20 (0.046)
Mean FD (mm), after scrubbing		0.14 ± 0.05	0.17 ± 0.06	0.002	-0.14 (0.1560)

(2014), and 57 subjects (32 HC) in Padula et al. (2015).

2.2. Image acquisition

Structural and functional MRI data were acquired at the Centre d'Imagerie BioMédicale (CIBM) in Geneva on a Siemens Trio (N=78) and a Siemens Prisma (N=22) 3 Tesla scanner. Anatomical images were acquired with a T1-weighted sequence of 0.86× 0.86×1.1 mm^3 volumetric resolution (192 slices, TR=2500 ms, TE=3 ms, acquisition matrix=224×256, field of view=22 cm^2, flip angle=8%), and functional images with a T2-weighted sequence of 8 minutes (voxel size=1.84×1.84×3.2 mm, 38 slices, TR=2400 ms, TE=30 ms, flip angle=85%). For the rs-fMRI session, participants were asked to fix a cross projected on a screen, let their minds wander while not thinking of anything in particular and not to fall asleep.

2.3. Preprocessing

Fig. 1 shows a graphical overview on our complete analysis, including rs-fMRI preprocessing steps. The rs-fMRI scans were preprocessed using Statistical Parametric Mapping (SPM12, Wellcome Trust Centre for Neuroimaging, London, UK: http://www.fil.ion.ucl.ac.uk/spm/). We adapted the pipeline of our previous studies (Richiardi et al., 2012; Scariati et al., 2014) and utilized functions of the Data Processing Assistant for Resting-State fMRI (DPARSF; Yan, 2010) and Individual Brain Atlases using Statistical Parametric Mapping (IBASPM; Aleman-Gomez et al., 2006) toolboxes. Functional images were realigned and spatially smoothed with an isotropic Gaussian kernel of 6 mm full width half maximum (FWHM). Structural scans were coregistered to the functional mean and segmented with the SPM12 *Segmentation* algorithm (Ashburner and Friston, 2005). A study-specific template was generated using Diffeomorphic Anatomical Registration using Exponentiated Lie algebra (DARTEL, Ashburner, 2007). After initial preprocessing, the voxelwise time series were extracted in individual subject space, excluding the first five time points, and the voxelwise time series were filtered with a bandwidth of 0.01 Hz to 0.1 Hz. Then, we applied motion scrubbing (Power et al., 2012) to correct for motion artifacts. Frames with high motion were marked according to the framewise displacement, which was calculated as the sum of the absolute values of the six realignment parameters (Power et al., 2012). Scans with a framewise displacement of more than 0.5 mm, as well as one scan before and two scans after, were excluded from the analysis.

2.4. BOLD signal variability

Voxelwise signal variability was determined by calculating the standard deviation (SD_{BOLD}) of preprocessed time series in subject space. According to Parseval's theorem, this approach is equivalent to the frequency-domain computation of the amplitude of low-frequency fluctuations (ALFF) at 0.01 Hz to 0.1 Hz.

Voxelwise BOLD variability maps were z-scored and warped to the study-specific DARTEL template by means of the nonlinear flow fields that were previously generated by the algorithm. We made the choice to apply spatial normalization on the variability maps, rather than the rs-fMRI data beforehand, as in this way voxel-wise measures such as ALFF are less affected by the spatial distortions (Wu et al., 2011).

2.5. Seed-based DMN functional connectivity

For DMN connectivity analysis, a seed region of 7× 7× 11 mm^3 was placed in the PCC at MNI coordinates [0, −56, 26] (Karahanoğlu and Van De Ville, 2015) and spatially transformed into the common space the study-specific DARTEL template. The seed region was then mapped into individual subject space and seed functional connectivity maps were calculated by computing the Pearson correlation coefficient of every voxel time course with the average time course inside the seed region. Voxelwise seed functional connectivity maps were z-scored for every subject and warped to the study-specific DARTEL template.

2.6. PLS correlation analysis

We applied PLS correlation (Krishnan et al., 2011; McIntosh and Lobaugh, 2004) to reveal alterations related to diagnosis and the relationship between brain measures and age. In the following, we are going to refer to subject-specific design variables (see also Fig. 1, yellow box).

For the current study, we included a variable corresponding to diagnosis (1 for HC, -1 for 22q11.2DS), age and age by diagnosis interaction as design variables in the PLS correlation analysis. As there were no significant effects of gender and its interaction with diagnosis when included in the analysis, here we only show the results for age and diagnosis. Only voxels with a probability higher than 0.5 of laying inside the gray matter of the study-specific DARTEL template were considered as brain data input. Prior to the application of PLS correlation, subject-specific design variables and voxelwise brain data

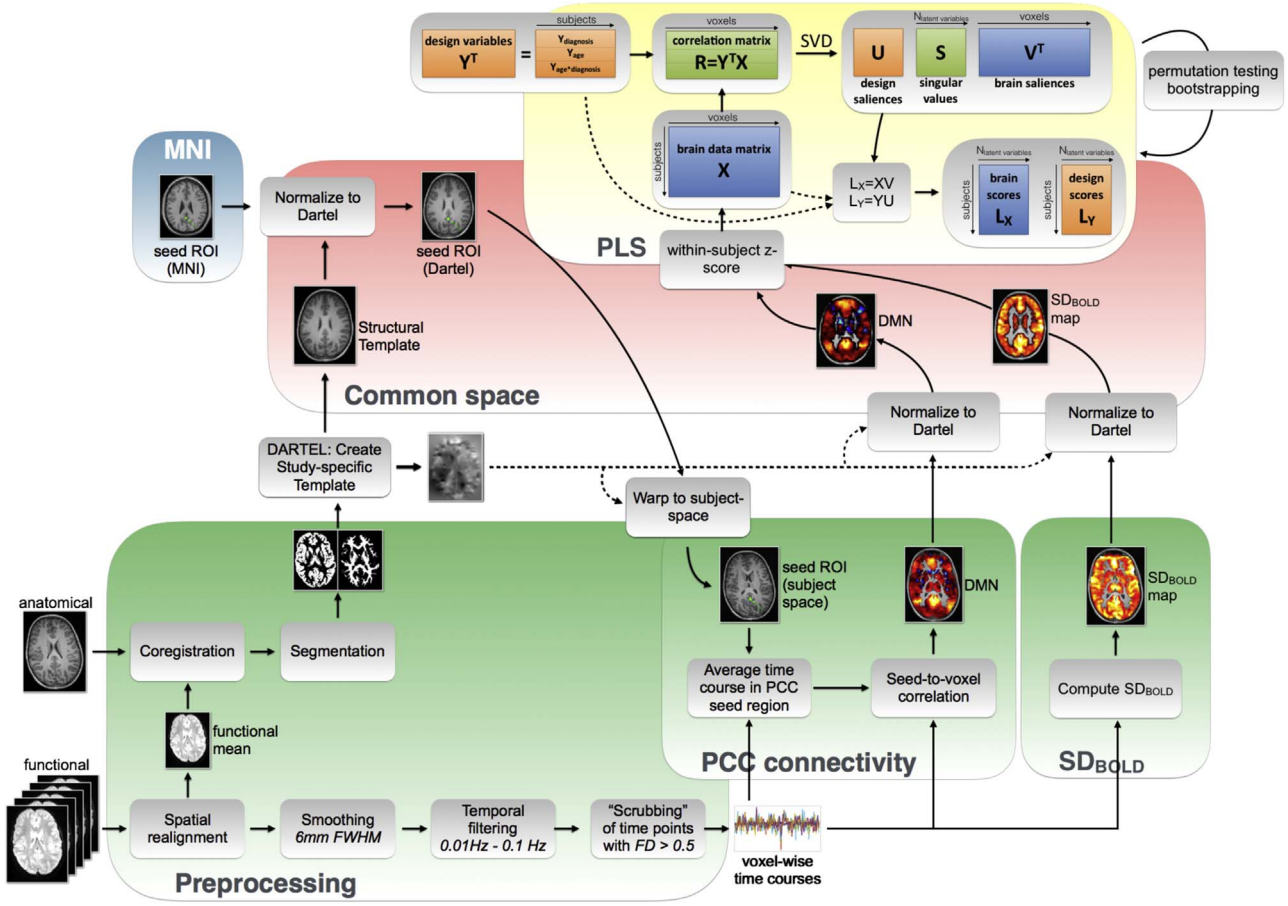

Fig. 1. Processing pipeline including preprocessing, computation of SD_{BOLD} and PCC connectivity, spatial normalization to a study-specific template created with DARTEL and PLS correlation analysis.

were z-scored across all subjects, as group information was already included in the first design variable.

The first step of PLS correlation is the computation of the correlation matrix $\mathbf{R} = \mathbf{X}^T\mathbf{Y}$ between a matrix of voxel data per subject $\mathbf{X}$ and a number of subject-specific design variables $\mathbf{Y}$. Here, we included the three design variables diagnosis, age and their interaction. Then, the singular value decomposition (SVD) of $\mathbf{R} = \mathbf{USV}^T$ produced three latent variables (LVs). Every LV is associated with 1) a singular value (diagonal elements of $\mathbf{S}$) indicating the correlation explained by that LV, 2) a vector of three left singular values $\mathbf{U}$, also called design saliences, and 3) a vector of right singular values $\mathbf{V}$, also called brain saliences or voxel saliences. The design saliences $\mathbf{U}$ indicate how strong each one of the three design variables contributes to the brain-design correlation explained by this LV. Similarly, the brain saliences $\mathbf{V}$ express how strong every voxel contributes to the brain-design correlation explained by this LV. Then, the projection of every subject's original brain data (in $\mathbf{X}$) onto the multivariate brain salience pattern (in $\mathbf{V}$) produces so-called "brain scores" $\mathbf{L_X} = \mathbf{XV}$. Those brain scores give a measure on the similarity of a subject's individual brain data with the salient brain pattern. Similarly, so-called "design scores" can be computed by $\mathbf{L_Y} = \mathbf{YU}$, which are a projection of every subject's design variables onto the respective design saliences.

In order to determine whether the explained correlation of every LV was significant, we applied permutation testing using 1000 permutations to determine the null distribution of the singular values. We applied Bonferroni correction for multiple comparisons when testing for significance of the three LVs. A LV was considered significant if the singular value was higher than 98.3% of its null distribution (p=0.017). If a LV was significant, we furthermore evaluated the robustness of brain and design saliences using a bootstrapping procedure with 500 random samples with replacement. Brain and design saliences were re-calculated for every bootstrap sample, resulting in a typical bootstrap distributing of the salience values. The division of the mean of this distribution by its standard deviation gives bootstrap scores for every voxel respectively design variable. Those bootstrap scores indicate the robustness of a voxel's response; i.e., its contribution to the voxelwise brain-behavior correlation and can be interpreted similarly to z-scores (Krishnan et al., 2011). In the results, we show the brain patterns of bootstrap scores thresholded at absolute values greater than 3.00, which corresponds to a robustness at a confidence level of approximately 99% (Garrett et al., 2013a). As there are only three design saliences per LV, a more detailed visualization than for the brain saliences is possible and we show the design salience bootstrap means as bar plots with error bars according to the bootstrap standard deviations.

2.7. Group-wise correlation of brain scores with age

In order to provide an alternative visualization of the results captured in the design saliences, we computed the correlation between brain scores and age in every group separately. In the results section, we plot the group-wise brain scores and their age-relationship in addition to the design saliences to facilitate the interpretation of those. P-values of the group-wise correlations were determined within the permutation loop during PLS correlation analysis.

2.8. Comparing brain salience patterns

In order to reveal similarities and differences in the patterns of voxel salience bootstrap scores in SD_{BOLD} and PCC connectivity, we

computed a joint map according to the magnitude and sign of the two brain maps. All voxels where the root mean square of bootstrap scores in both maps exceeded 3 were included into the joint map. Remaining voxels were colored according to the angle between SD_{BOLD} bootstrap scores and PCC connectivity bootstrap scores. This allowed us to combine the following cases in one single map: 1) Areas where either *only* SD_{BOLD} or *only* PCC connectivity are altered, color-coded according to the direction of that alteration (four cases: only SD_{BOLD} higher/lower, only PCC connectivity higher/lower). 2) Areas where *both* SD_{BOLD} and functional connectivity are altered, color-coded according to the direction of that alteration (four cases: both higher, both lower, SD_{BOLD} higher and PCC connectivity lower, SD_{BOLD} lower and PCC connectivity higher).

3. Results

PLS correlation analysis of voxelwise SD_{BOLD} resulted in two significant LVs. The first significant LV ($p < 0.001$) captured mainly effects of diagnosis of the SD_{BOLD}-design correlation, the corresponding brain saliences can thus be interpreted similarly to a multivariate contrast between patients and controls. The second significant LV (p=0.001) captured mainly age-effects in the SD_{BOLD}-design relationship and almost no effect of diagnosis. The corresponding brain saliences thus represents voxels which are strongly correlated with age in both groups.

PLS correlation analysis of seed-to-voxel PCC connectivity resulted in only one significant LV ($p < 0.001$) which captured both a strong effect of diagnosis *and* age. The corresponding brain salience pattern shows thus voxels which are different in patients compared to controls, but where PCC connectivity is also correlated with age in both groups.

In the following section, we show the PLS correlation results for SD_{BOLD} and PCC connectivity in more detail. The first subsection describes results obtained in SD_{BOLD}, the second subsection describes results obtained in PCC connectivity and in the third subsection, we provide a comparison of the two previous results by showing an overview on the similarities and differences between the brain salience patterns of the first (mainly diagnosis-related) LV of SD_{BOLD} and the first (both diagnosis- and age-related) LV of PCC connectivity.

3.1. SD_{BOLD}

In this subsection, we first show the average SD_{BOLD} maps in our cohort, then describe the first (mainly diagnosis-related) significant LV that results from the PLS correlation analysis of SD_{BOLD}, and conclude with a description of the second (mainly age-related) significant LV.

3.1.1. SD_{BOLD}: average across all subjects

Fig. 2 shows the average SD_{BOLD} across all subjects. SD_{BOLD} is very strong in medial regions of the DMN, such as the PCC, precuneus and the medial prefrontal cortex. There was no significant group difference in the within-subject average SD_{BOLD} which was subtracted during z-scoring (two sample t-test, p=0.195).

3.1.2. SD_{BOLD}: LV1 reflects a main effect of diagnosis

Fig. 3a to c show brain and design saliences corresponding to the first significant LV ($p < 0.001$) for PLS correlation analysis of SD_{BOLD}. There is a very strong effect of diagnosis (design salience 0.96 ± 0.04) a small negative effect of age (design salience -0.16 ± 0.08), as well as a negative effect of age by diagnosis interaction (design salience -0.23 ± 0.07).

Correlation plots of brain scores with age are shown on Fig. 3b. In HCs, brain scores are significantly negatively correlated with age (ρ=-0.58, p=0.001), whereas in the patients group there is no significant correlation (ρ=0.09, p=0.626). This means that in brain areas with positive resp. negative bootstrap scores (red resp. blue), SD_{BOLD} is negatively resp. positively correlated with age in controls but not in patients.

Due to the high diagnosis salience, the corresponding pattern of brain salience bootstrap scores (see Fig. 3c) can be interpreted as a multivariate contrast showing areas of higher (red) and lower (blue) SD_{BOLD} in 22q11.2DS. Reduced SD_{BOLD} can be found in regions of the DMN such as PCC, lateral parietal and medial prefrontal cortices, as well as in the dorsal anterior cingulate and the dorso-lateral prefrontal cortices. SD_{BOLD} is bilaterally elevated in the inferior temporal cortex including parahippocampus, in the superior temporal gyrus and in caudate.

3.1.3. SD_{BOLD}: LV2 reflects a main effect of age

Brain and design saliences of the second significant LV (p=0.001) are shown on Fig. 3d to f. There are a strong age effect (design salience 0.99 ± 0.07) and a small effect of diagnosis (design salience 0.16 ± 0.09). However, no significant effect of age by diagnosis interaction appeared (design salience -0.01 ± 0.14).

Group-wise correlation analysis between brain scores and age (see Fig. 3e) shows strong correlation values in both groups, as was expected based on the high age salience without interaction salience. Overall brain scores are slightly higher in patients (small diagnosis salience).

Due to the high age salience, the corresponding pattern of brain salience bootstrap scores (see Fig. 3f) contains the voxels where SD_{BOLD} is strongly correlated with age in both patients and controls. SD_{BOLD} increases over age in the dorsal anterior cingulate cortex, superior frontal cortex, as well as parts of thalamus. Small clusters with decreasing SD_{BOLD} are located in the anterior cingulate and orbitofrontal cortices.

3.2. PCC functional connectivity

This subsection begins with the average PCC connectivity maps, followed by a description of the only significant (both diagnosis- and age-related) significant LV resulting from PLS correlation analysis of PCC connectivity.

3.2.1. PCC connectivity: average across all subjects

Fig. 4 shows the average PCC connectivity across all subjects. As expected regions of the DMN are strongly positively correlated with the PCC, while there is a weaker, negative correlation with regions of the frontoparietal network, consisting of lateral frontal and parietal regions. There was no significant group difference in the within-subject average connectivity which was subtracted z-scoring (two sample t-test, p=0.959).

3.2.2. PCC connectivity: LV1 reflects effects of both diagnosis and age

The brain bootstrap scores as well as the corresponding design saliences for the first significant LV ($p < 0.001$) are shown on Fig. 5a to c. There is a very high effect of diagnosis (design salience 0.91 ± 0.06) meaning that corresponding brain voxel saliences can be interpreted as a multivariate pattern of altered DMN connectivity in 22q11.2DS. Additionally, there is a moderate negative effect of age (design salience -0.38 ± 0.08) and a small interaction between age and diagnosis (design salience 0.16 ± 0.08).

As already indicated by the design saliences, group-wise correlation of brain scores with age (see Fig. 5b) shows that brain scores are significantly negatively correlated with age in both groups, but the negative correlation is stronger in patients (small interaction effect).

Due to the high diagnosis salience value, the corresponding pattern of brain salience bootstrap scores (see Fig. 5c) can be interpreted as a multivariate contrast showing areas of higher (red) and lower (blue) PCC connectivity in 22q11.2DS. The negative age salience indicates that PCC connectivity in the brain salience pattern is furthermore negatively (red) and positively (blue) correlated with age.

Regions of elevated PCC connectivity in patients include the middle frontal and inferior parietal cortices, regions of the frontoparietal or

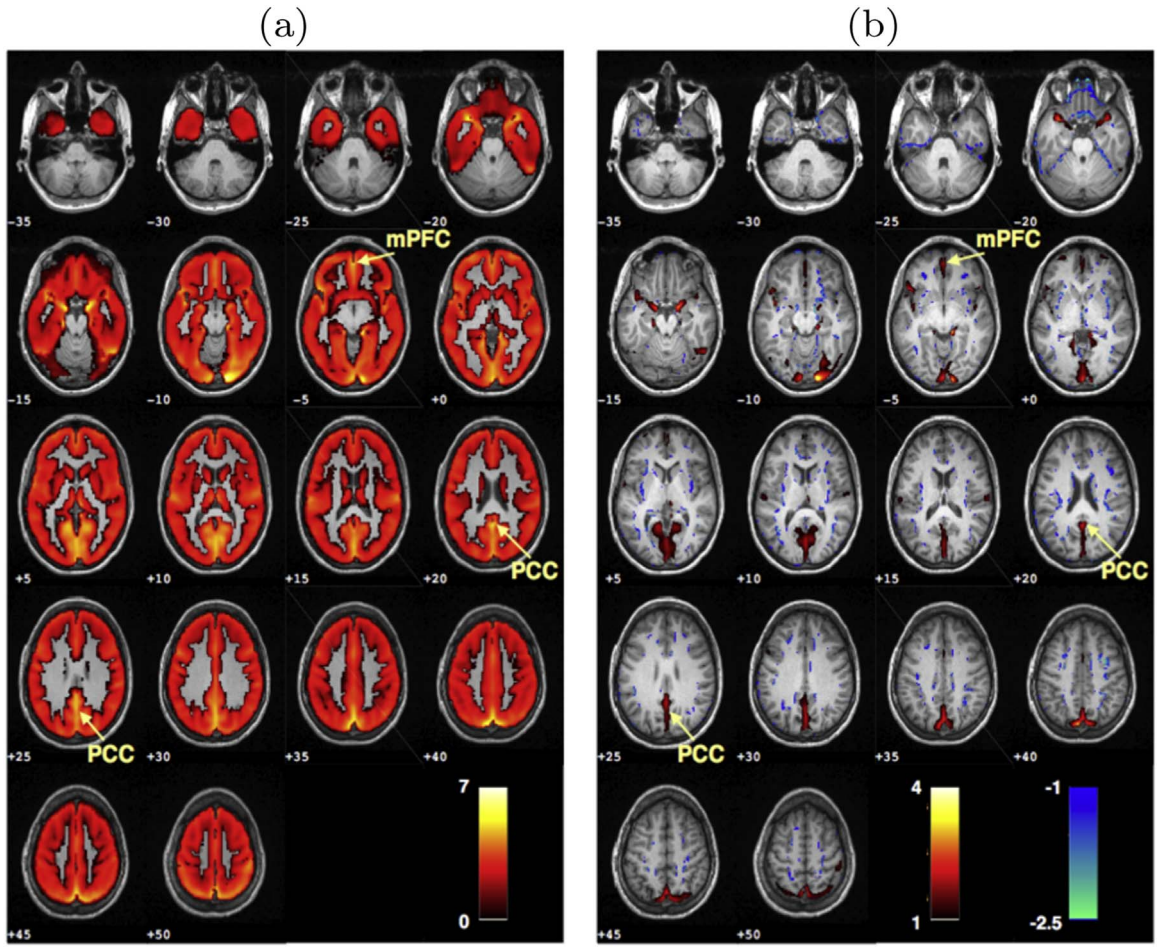

Fig. 2. Average SD_{BOLD} in gray matter, (a) original values (b) within-subject z-scores. mPFC - medial prefrontal cortex; PCC - posterior cingulate cortex.

central executive network which is in fact negatively correlated with the DMN. Thus, we can derive that the anti-correlation between the PCC and the frontoparietal network is weaker in 22q11.2DS.

Reduced PCC connectivity can be observed in the medial prefrontal cortex, confirming previous observations on long-range anterior-posterior DMN dysconnectivity (Schreiner et al., 2014; Padula et al., 2015). PCC functional connectivity towards the anterior cingulate cortex and posterior insula, areas of the salience network, is also lower in 22q11.2DS.

3.3. *Comparison of* SD_{BOLD} *and PCC connectivity alterations*

The first LV has a strong diagnosis salience in both SD_{BOLD} and PCC connectivity. In order to compare the two patterns of alterations in 22q11.2DS, we computed the joint map between the brain salience bootstrap score maps of the two measures (see Fig. 6). In some regions either only SD_{BOLD} or only PCC connectivity are altered. Most areas in the inferior temporal lobe have only higher SD_{BOLD} while PCC connectivity is not altered (red), while in the gyrus rectus only PCC connectivity is altered. In medial regions of the DMN (precuneus and medial prefrontal cortex) and in the middle temporal gyrus, both measures are reduced. Interestingly there are no areas where both measures are significantly elevated in 22q11.2DS. In the frontoparietal network, SD_{BOLD} is lower and PCC connectivity higher in 22q11.2DS (bluish green). As stated in the previous paragraph, PCC connectivity in those areas has negative values; higher connectivity thus indicates a weaker correlation. Interestingly, in most regions where both measures are altered, SD_{BOLD} is reduced. Elevated SD_{BOLD} seemingly has not driven any reductions in PCC functional connectivity.

4. Discussion

In the present study we employed multivariate PLS correlation to reveal altered brain function and age-relationship in 22q11.2DS. We used two different approaches to analyze resting-state BOLD signals: BOLD signal fluctuations assessed by the standard deviation of every voxel's temporal signal and seed-based functional connectivity between the PCC and the other brain voxels. With both approaches we were able to reveal multivariate patterns of altered brain function in 22q11.2DS. In both measures, the first significant LV was representing areas of altered brain function related to 22q11.2DS. In SD_{BOLD}, there was also an effect of age by diagnosis interaction in the first LV, suggesting an altered developmental trajectory of SD_{BOLD} in those areas. In SD_{BOLD} there was a second age-related brain pattern, which revealed the brain regions with the strongest age-relationship in both groups. The corresponding pattern was not overlapping with the pattern of the first LV and patients had the same developmental curve as controls in those areas. In PCC connectivity, the pattern of alterations corresponding to LV1 was also correlated with age, but PLS correlation revealed no separate age-related component as in SD_{BOLD}.

In the following, the two significant LVs for SD_{BOLD} and the only significant LV for PCC connectivity will be discussed one after another. Finally, the relationship between SD_{BOLD} and functional connectivity will be examined on the basis of the comparison between the patterns of altered brain function.

4.1. SD_{BOLD} *alterations in 22q11.2DS*

To our best knowledge, this is the first study to date analyzing

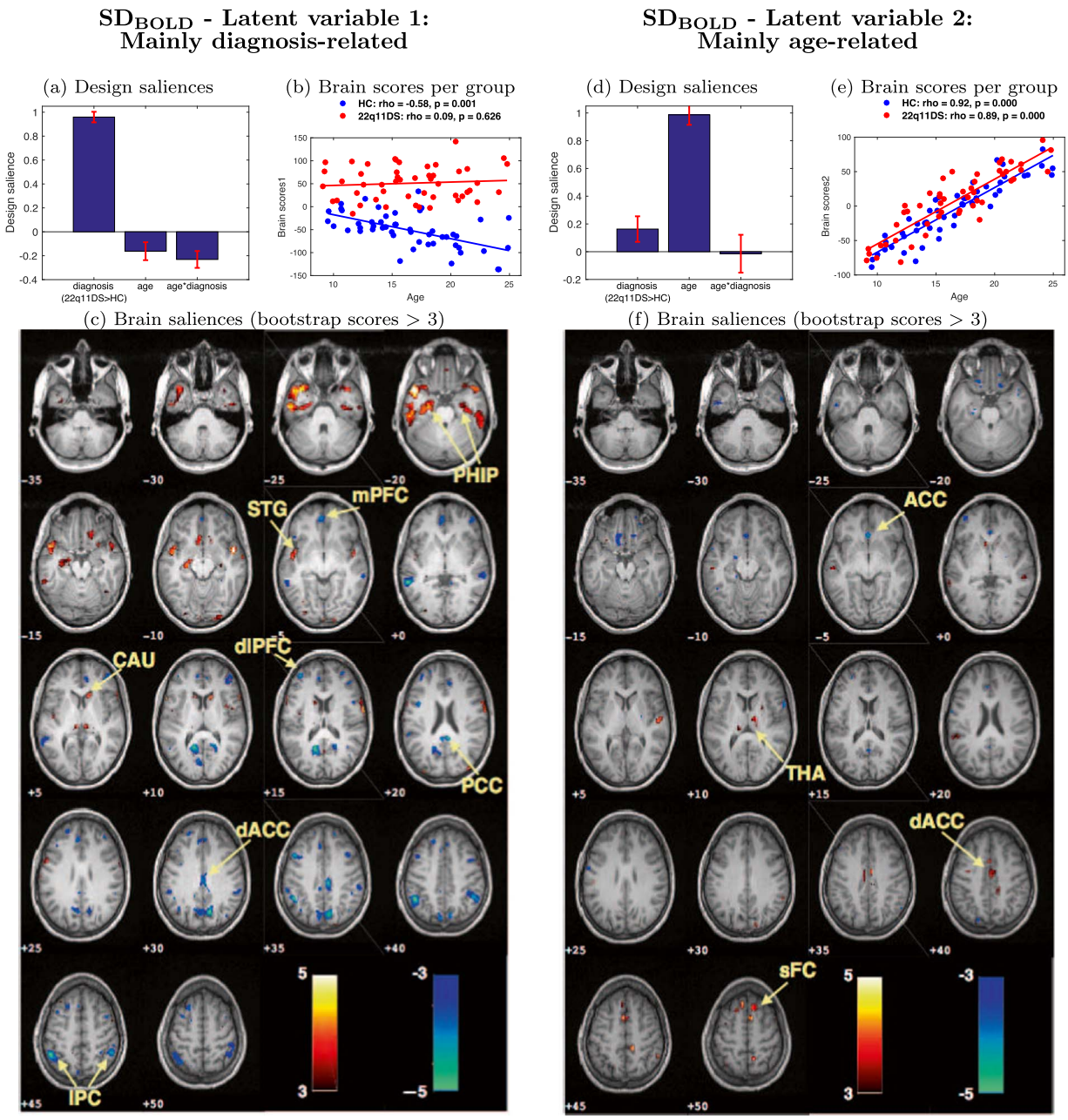

Fig. 3. SD_{BOLD}: PLS correlation analysis results in two significant LVs. Left column: (a) The design saliences of the first LV reveal a strong effect of diagnosis, almost no age effect and a negative age by diagnosis effect. (b) Separate correlation of brain scores with age in every group gives an alternative view of those results: Brain scores are higher in 22q11.2DS (diagnosis-effect) and are negatively correlated with age in HC but not in 22q11.2DS (negative age- and interaction-effects). (c) The first pattern of brain saliences can thus be interpreted as multivariate contrast. Areas with robustly lower SD_{BOLD} in 22q11.2DS (blue) are mainly part of the DMN (PCC, IPL, mPFC), and also include medial (dACC) and lateral prefrontal (dlPFC) regions. Clusters with robustly higher SD_{BOLD} (red) are located in the inferior temporal lobes including PHIP, as well as in the STG and CAU. Right column: (d) The design saliences of the second LV reveal a strong age-effect across all subject, as well as a small effect of diagnosis, but no interaction. (e) Separate correlation between brain scores and age in every group shows again the strong relationship with age in both controls and patients. Brain scores are slightly higher in patients, as already indicated by the small positive diagnosis design salience. (f) The second pattern of brain saliences shows thus voxels which are robustly correlated with age in both groups. Regions with positive age-relationship (red) are located in THA, dACC and the sFC, while in a small cluster in the ACC (blue), SD_{BOLD} is negatively correlated with age. ACC - anterior cingulate cortex; CAU - caudate; dACC - dorsal ACC; dlPFC - dorso-lateral prefrontal cortex; IPC - inferior parietal cortex; mPFC - medial prefrontal cortex; PCC - posterior cingulate cortex; PHIP - parahippocampus; sFC - superior frontal cortex; STG - superior temporal gyrus; THA - thalamus.

moment-to-moment BOLD signal variability in 22q11.2DS. During our first analysis we showed that z-scored SD_{BOLD} is altered in a broad pattern, showing both elevated and reduced SD_{BOLD} in patients with 22q11.2DS (LV1, see Fig. 3c). SD_{BOLD} is lower in large parts of the DMN including the medial prefrontal cortex, PCC, and lateral parietal cortex. A previous study on BOLD variability during task in healthy adults found decreased variability in an elderly, low performing group compared to young adults in a very similar set of brain regions (Garrett et al., 2011). Alterations in lateral parietal regions might be implicated in visuospatial processing difficulties of patients with 22q11.2DS (Gothelf et al., 2008), while the PCC and precuneus have been identified as structural and functional network hubs, associated with self-referential processes and theory of mind (van den Heuvel and Sporns, 2013; Spreng et al., 2008). Another cluster of reduced SD_{BOLD} is located in the dorso-lateral prefrontal cortex, a region which is known to be structurally and functionally affected in schizophrenia (Jung et al., 2010; Sun et al., 2009; Karlsgodt et al., 2014). In 22q11.2DS, structural MRI studies have shown relative reductions of

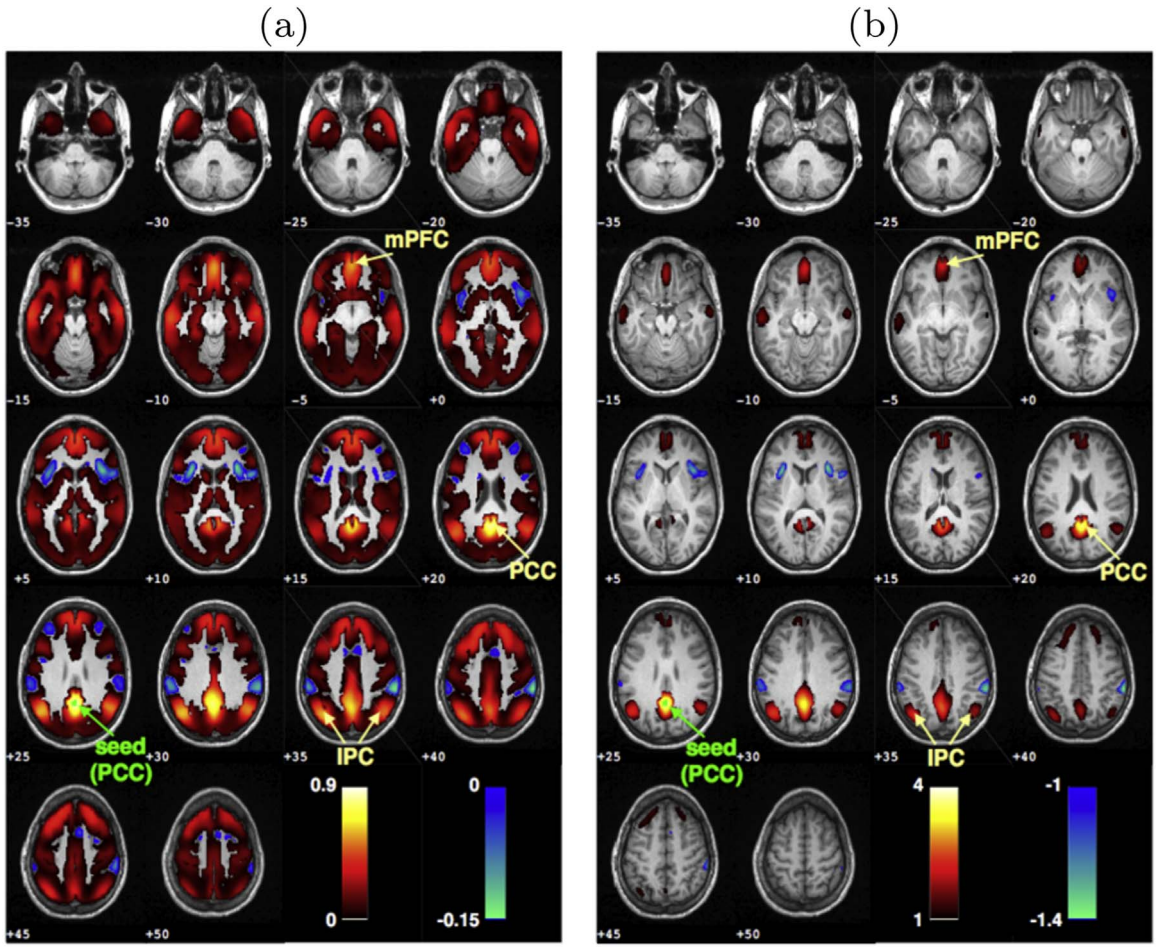

Fig. 4. Average PCC connectivity, (a) original values (b) within-subject z-scores. IPC - inferior parietal cortex; mPFC - medial prefrontal cortex; PCC - posterior cingulate cortex; seed - region of interest in the posterior cingulate cortex.

cortical volume and thickness in the parietal cortex, the dorso-lateral prefrontal cortex and along midline structures (Schmitt et al., 2015; Gothelf et al., 2008; Jalbrzikowski et al., 2013). The similarity to the here observed pattern of BOLD variability reductions suggests a link between altered cortical volume and BOLD signal variability alterations.

Additionally, we observed a significant relationship with age in regions with altered SD_{BOLD} in HCs, but not in the 22q11.2DS group (see Fig. 3a and b). More specifically, brain scores decrease over age in controls whereas in patients, they are not correlated with age. This observation suggests that elevated and reduced SD_{BOLD} might be caused by altered developmental trajectories in patients with 22q11.2DS. Developmental alterations in 22q11.2DS have already been observed in several other modalities (Schaer et al., 2009; Padula et al., 2015; Gothelf et al., 2008; Shashi et al., 2012; Jalbrzikowski et al., 2013), including deviant maturation curves of cortical thickness (Schaer et al., 2009) and structural connectivity (Padula et al., 2015).

4.2. SD_{BOLD} development

We furthermore showed that, in a different set of brain regions, SD_{BOLD} is strongly correlated with age, both in 22q11.2DS and HCs (LV2, see Fig. 3f). More specifically, BOLD variability increases with age in most of the regions showing a robust age-effect, namely thalamus, dorsal anterior cingulate and superior frontal cortex. In those regions, older subjects of our cohort had higher SD_{BOLD} than children. In one cluster of the anterior cingulate cortex and bilaterally in the orbitofrontal cortex, SD_{BOLD} was robustly decreasing over age. Garrett et al. (2013b) suggested that brain signal variability follows an inverted U-shaped curve over life-span, increasing from child- to young adulthood and decreasing again with higher age. In the present study, we observed mainly increasing SD_{BOLD} from child- to young adulthood, a result which is in line with the previously stated hypothesis. However, Garrett et al. based their hypothesis within the age range from child- to adulthood only on task-based EEG (McIntosh et al., 2008; Lippé et al., 2009) and MEG studies (Misić et al., 2010). Here we provide additional information to those results in our cohort using rs-fMRI. Increasing variability suggests the transition towards a system of higher dynamic complexity that has greater adaptability, efficiency and dynamic range leading to enhanced cognitive function (Misić et al., 2010; Deco et al., 2011; Ghosh et al., 2008; Garrett et al., 2013b). Interestingly, the areas showing robust relationship with age are not overlapping with the pattern of SD_{BOLD} alterations. Patients have normally developing BOLD signal variability in those areas.

4.3. PCC connectivity alterations in 22q11.2DS

In order to compare the effects of BOLD signal variability with conventional functional connectivity, we studied seed-based connectivity within the DMN. The DMN is one of the most studied RSNs and two studies to date explicitly studied DMN functional connectivity in 22q11.2DS using different seed-based approaches (Schreiner et al., 2014; Padula et al., 2015). Padula et al. (2015) found reduced connectivity between anterior-posterior nodes of the DMN, as well as between right and left parietal lobes. Schreiner et al. (2014) used a very

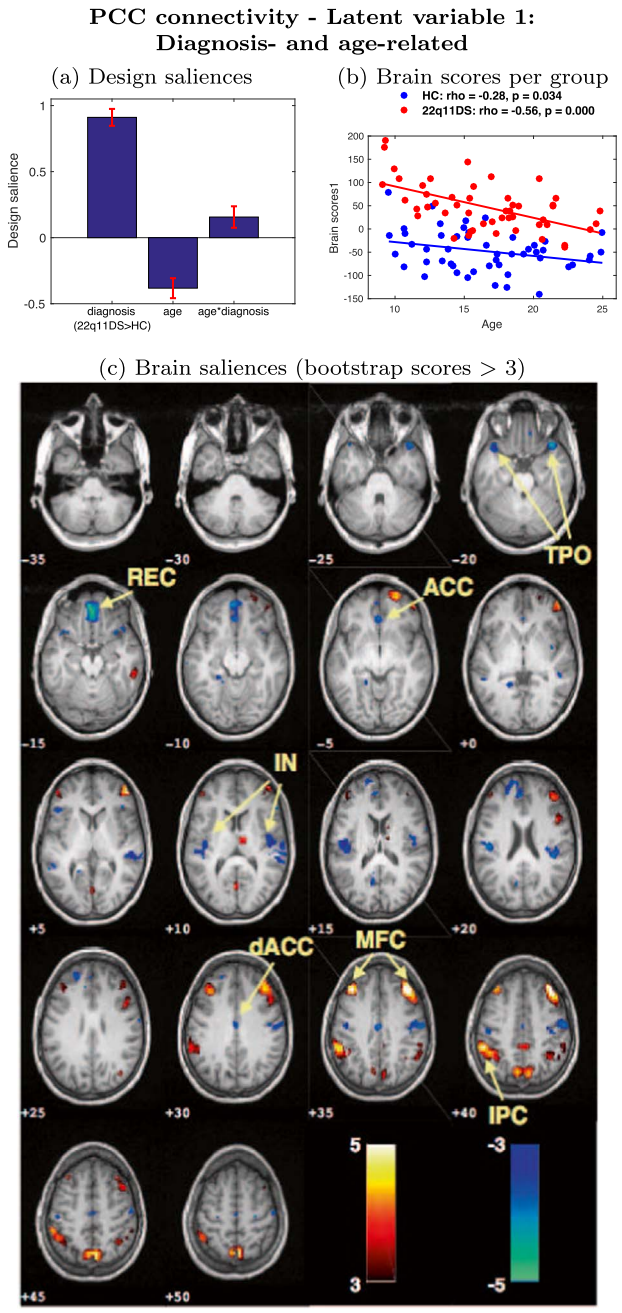

Fig. 5. PCC connectivity: PLS correlation analysis results in one significant LV. (a) The design saliences of the LV reveal a strong positive effect of diagnosis, as well as a moderate negative age-effect and a small positive effect of interaction. (b) Separate correlation of brain scores with age in every group gives an alternative view on those results: Brain scores are higher in 22q11.2DS (diagnosis-effect) and are negatively correlated with age (negative age-effect) in both groups. The correlation is stronger in patients than in controls (interaction-effect) (c) The pattern of brain saliences can thus be interpreted as areas of higher (red) and lower (blue) PCC connectivity in 22q11.2DS, where PCC connectivity is also negatively (red) and positively (blue) correlated with age. PCC connectivity in 22q11.2DS is higher (red) in the frontoparietal network (IPC and MFG). PCC connectivity in 22q11.2DS is lower (blue) in the posterior insula and the ACC, as well as in the TPO and REC. ACC - anterior cingulate cortex; dACC - dorsal ACC; IN - insula; IPC - inferior parietal cortex; MFC - middle frontal cortex; REC - gyrus rectus; TPO - temporal poles.

similar approach to ours in an independent sample, analyzing voxel-wise connectivity of a seed placed in the PCC. They found globally lower within-DMN connectivity and higher connectivity between the PCC and the right inferior frontal gyrus.

In the present study we were able to confirm the lower anterior-posterior connectivity within the DMN between PCC and the medial prefrontal and left superior frontal cortices (LV1, see Fig. 5c). However, thanks to our multivariate approach, we obtained a much broader pattern of altered PCC connectivity. In particular, we found lower connectivity with the temporal poles, an effect that has also been observed in schizophrenia with a relationship to self-disturbance and hallucinations (Pankow et al., 2015).

Furthermore we observed weaker anti-correlation between the PCC and the frontoparietal network, a network playing a central role in working memory and attention. It has been proposed that switching between the DMN, the frontoparietal network and the saliency network is crucial for normal brain functioning and that dysconnectivity between those networks plays a central role in multiple psychopathologies (Menon, 2011; Menon and Uddin, 2010) and schizophrenia in particular (Hasenkamp et al., 2011).

Our observation on broad dysconnectivity between the DMN and frontoparietal network in our cohort of 22q11.2DS patients, supports the hypothesis of a strong implication in psychiatric disorders.

To date, only one study has analyzed the development of DMN connectivity over age in 22q11.2DS (Schreiner et al., 2014), reporting increased long-range connectivity within the DMN in controls and abnormally increasing PCC connectivity with regions outside the DMN in patients. Our approach in the present study is complementary, as our PLS approach optimizes for a maximum age correlation in *all* subjects, independently of the diagnosis. The age-relationship of the mainly diagnosis-related LV1 supports increasing within-DMN connectivity. However, we did not observe any effect of interaction between age and diagnosis.

4.4. PCC connectivity development

In PCC connectivity, there was no significant second LV as in the analysis of SD_{BOLD}, indicating that all developmental effects of DMN connectivity were already explained by the first LV. In the first LV, PCC connectivity was correlated with age in both groups, but stronger in patients (see Figs. 5a and b). As most studies focus only on maturation effects *within* the DMN without taking into account the whole brain (for instance Sherman et al., 2014 and Supekar et al., 2010) those results are difficult to confirm and further analysis will be necessary to get more insight in the underlying effects.

4.5. Relationship of SD_{BOLD} and functional connectivity

Overall, we showed that alterations in SD_{BOLD} might be explained by altered developmental trajectories in 22q11.2DS, while in PCC connectivity both groups show a strong relationship with age. Furthermore, the second significant LV in SD_{BOLD}, which represents strong age-relationship in all subjects, is absent in PCC connectivity, suggesting that SD_{BOLD} is stronger implicated in development. These findings confirm existing literature emphasizing BOLD signal variability as a promising tool for the analysis of brain development and its alterations in neurodevelopmental disorders (Garrett et al., 2013b; McIntosh et al., 2010), which is complementary to functional connectivity analysis.

Furthermore, there is a close relationship between SD_{BOLD} and functional connectivity, as the standard deviation appears in the denominator of the Pearson correlation coefficient (Garrett et al., 2013b; Zalesky et al., 2012):

$$\rho_{xy} = \frac{\sum (x - \bar{x})(y - \bar{y})}{SD_x SD_y} \quad (1)$$

Thus, alterations of functional connectivity might actually be driven by alterations of covariance in the numerator or by variance in the denominator. In the present study we addressed this question based on the analysis of the DMN as one exemplary RSN. We showed that

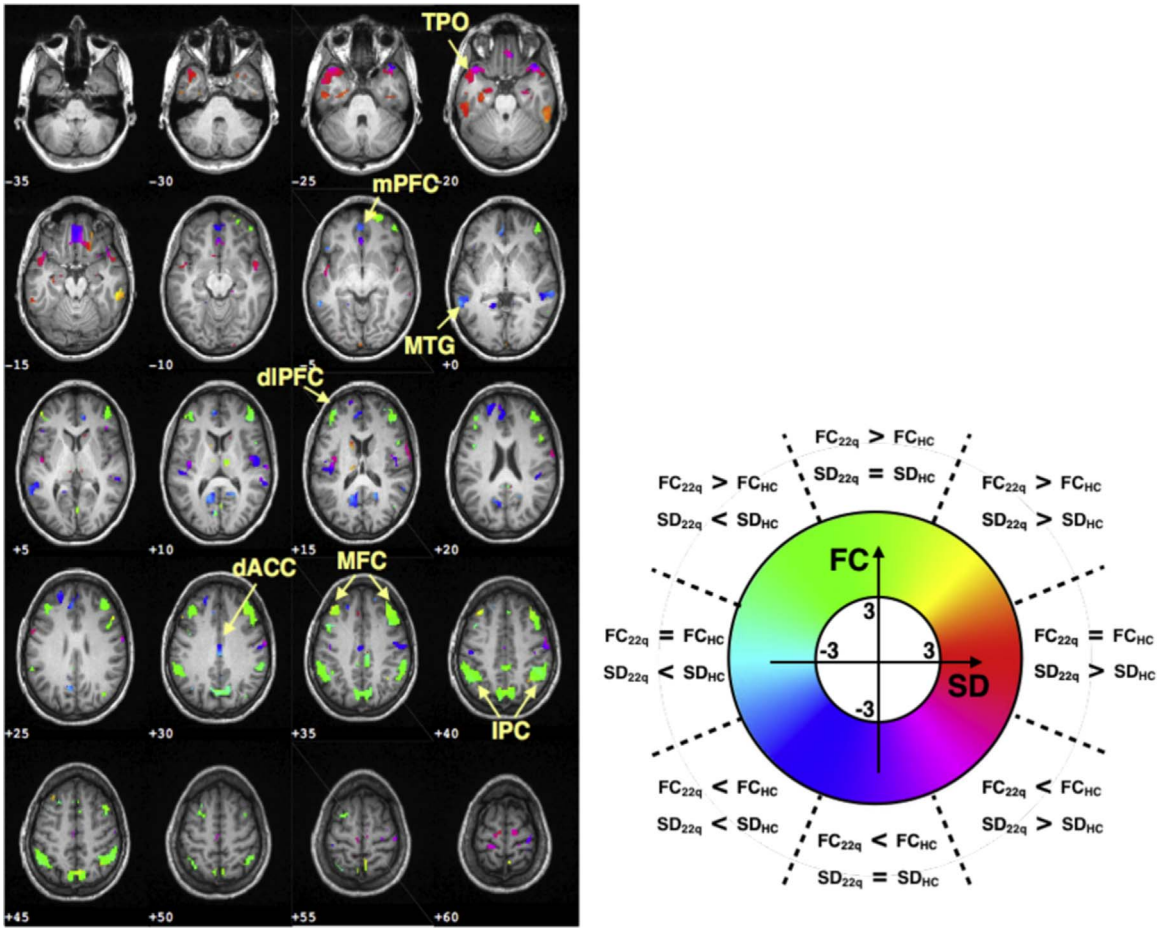

Fig. 6. Joint map between SD_{BOLD} LV1 bootstrap scores (see Fig. 3c) and PCC connectivity LV1 bootstrap scores (see Fig. 5c). Color codes indicated whether only one measure is altered in 22q11.2DS or both and in which direction. In the frontoparietal network, SD_{BOLD} is lower and PCC connectivity higher in 22q11.2DS (bluish green). In medial regions of the DMN (mPFC, precuneus) both are reduced. Interestingly, in areas with elevated SD_{BOLD} (inferior temporal lobe), PCC connectivity is mostly not altered. IPC - inferior parietal cortex; dACC - dorsal anterior cingulate cortex; dlPFC - dorso-lateral prefrontal cortex; MFC - middle frontal cortex; mPFC - medial prefrontal cortex; MTG - middle temporal gyrus; TPO - temporal poles; *FC - functional connectivity; SD - BOLD signal standard deviation* (SD_{BOLD}).

lower functional connectivity of the PCC is not driven by higher SD_{BOLD}, but that in the areas where both are altered, SD_{BOLD} is also lower and thus covariance has to be lower to an even stronger extent than the correlation. Future analysis including more RSNs and whole brain functional connectivity may give further insight into this question.

5. Methodological considerations

5.1. PLS correlation analysis

We employed multivariate PLS correlation analysis to investigate diagnosis-related alterations and the age-relationship of SD_{BOLD} and functional connectivity of the DMN. We chose this approach because conventional GLM analysis, and also other multivariate approaches such as multivoxel pattern analysis (MVPA, De Martino et al., 2008) or multivariate distance matrix regression (MDMR, Zapala and Schork, 2006) have the limitation that we obtain only one brain map per included regressor, which indicates how strong that regressor is related to the response variable (here SD_{BOLD}). PLS correlation instead searches to explain the most variance as possible between distributed patterns of brain data and a *combination* of regressors. Its great advantage compared to other multivariate approaches is thus the possibility to investigate the relationship of brain data with multiple external variables at the same time. Here, this approach allowed us to investigate alterations related to 22q11.2DS *and* developmental characteristics *at the same time*. However, the multivariability of both brain and design saliences also introduces challenges the interpretability of the results.

5.2. SD_{BOLD} and motion

In the analysis of functional connectivity, but even more in SD_{BOLD}, motion is a known issue, as high changes in the BOLD signal might be caused by sudden motion (Power et al., 2012, 2014). Clinical populations, such as our cohort of patients with 22q11.2DS who present both mental and psychiatric disorders, move more than healthy subjects. This makes it is especially difficult to disentangle effects which are solely driven by motion. Here, we addressed this issue by excluding extreme motion outliers during preprocessing. After motion scrubbing, the framewise displacement was significantly higher in patients compared to controls, while the mean translation and rotation parameters did not differ between the groups. As this difference in motion is inherent to the clinical population under study, it is very difficult to obtain a perfect match between patients and controls without selecting a subpopulation of patients. Even though we applied strict motion correction, this effect presents still a limitation to our study. A more detailed analysis of the association between SD_{BOLD} and motion can be found in the Supplementary Material.

6. Conclusions and outlook

In this study we showed that BOLD signal variability is broadly altered in 22q11.2DS, strongest in regions of the DMN. We moreover observed that SD_{BOLD} is strongly related to age in a set of mainly subcortical brain regions. The locations and comparison to studies on BOLD variability during task suggest an implication of higher BOLD signal variability for better cognitive performance. However, further targeted studies including behavioral variables and task-based fMRI will be necessary to obtain a better understanding on the relationship on BOLD signal variability and behavior. Furthermore, we note that areas showing altered BOLD signal variability are reported to be also structurally affected in 22q11.2DS. The direct link between BOLD variance and brain anatomy should thus be subject to further analysis.

In an attempt to study the relationship between SD_{BOLD} and functional connectivity, we analyzed functional connectivity within the DMN and identified locations where functional connectivity might be confounded by brain variability. However, as we only studied connectivity of one seed region located in the PCC, the conclusions that can be driven are limited to this particular network. Further analysis should also include other RSNs or whole-brain connectivity approaches.

Conflict of interest

The authors declare no conflicts of interest.

Acknowledgements

We are grateful to the families who participated in our study and thank Sarah Menghetti and Léa Chambaz for their involvement with the families. We furthermore would like to acknowledge François Lazeyras and the group of CIBM for their support during data collection and Frédérique Bena Sloan for the genetic analysis.

This research was supported by the Swiss National Research Foundation (SNF) [grant numbers 32473B_121996, 234730_144260 to S. Eliez, and PP00P2_146318 to D. Van De Ville]. It was also supported by the National Center of Competence in Research (NCCR) “SYNAPSY – The Synaptic Bases of Mental Diseases” [SNF, grant number 51AU40_125759 to S. Eliez], as well as individual grants of the SNF to S. Eliez [grant number #145250] and M. Schaer [grant number #145760].

Appendix A. Supplementary data

Supplementary data associated with this article can be found in the online version at http://dx.doi.org/10.1016/j.neuroimage.2017.01.064.

References

Aleman-Gomez, Y., Melie-García, L., Valdés-Hernandez, P. 2006. IBASPM: toolbox for automatic parcellation of brain structures. In: Proceedings of the 12th Annu. Meet. Organ. Hum. Brain Mapp.

Allen, E.A., Damaraju, E., Plis, S.M., Erhardt, E.B., Eichele, T., Calhoun, V.D., 2014. Tracking whole-brain connectivity dynamics in the resting state. Cereb. Cortex 24, 663–676. http://dx.doi.org/10.1093/cercor/bhs352.

Antshel, K.M., Fremont, W., Kates, W.R., 2008. The neurocognitive phenotype in velo-cardio-facial syndrome: A developmental perspective. Dev. Disabil. Res. Rev. 14, 43–51. http://dx.doi.org/10.1002/ddrr.7.

Ashburner, J., Friston, K.J., 2005. Unified segmentation. Neuroimage 26, 839–851. http://dx.doi.org/10.1016/j.neuroimage.2005.02.018.

Ashburner, J., 2007. A fast diffeomorphic image registration algorithm. Neuroimage 38, 95–113. http://dx.doi.org/10.1016/j.neuroimage.2007.07.007.

Bassett, A.S., Chow, E.W.C., 1999. 22q11 deletion syndrome: a genetic subtype of schizophrenia. Biol. Psychiatry 46, 882–891. http://dx.doi.org/10.1016/S0006-3223(99)00114-6.

Davis, T., LaRocque, K.F., Mumford, J.A., Norman, K.A., Wagner, A.D., Poldrack, R.A., 2014. What do differences between multi-voxel and univariate analysis mean? How subject-, voxel-, and trial-level variance impact fMRI analysis. Neuroimage 97, 271–283. http://dx.doi.org/10.1016/j.neuroimage.2014.04.037, (URL ⟨http://dx.doi.org/10.1016/j.neuroimage.2014.04.037⟩).

De Martino, F., Valente, G., Staeren, N., Ashburner, J., Goebel, R., Formisano, E., 2008. Combining multivariate voxel selection and support vector machines for mapping and classification of fMRI spatial patterns. Neuroimage 43, 44–58. http://dx.doi.org/10.1016/j.neuroimage.2008.06.037.

Debbané, M., Lazouret, M., Lagioia, A., Schneider, M., Van De Ville, D., Eliez, S., 2012. Resting-state networks in adolescents with 22q11.2 deletion syndrome: associations with prodromal symptoms and executive functions. Schizophr. Res. 139, 33–39. http://dx.doi.org/10.1016/j.schres.2012.05.021, (URL ⟨http://linkinghub.elsevier.com/retrieve/pii/S0920996412003143⟩).

Deco, G., Jirsa, V.K., McIntosh, A.R., 2011. Emerging concepts for the dynamical organization of resting-state activity in the brain. Nat. Rev. Neurosci. 12, 43–56. http://dx.doi.org/10.1038/nrn2961, (URL ⟨http://www.dx.doi.org/10.1038/nrn2961⟩).

Di Martino, A., Yan, C.-G., Li, Q., Denio, E., Castellanos, F.X., Alaerts, K., Anderson, J.S., Assaf, M., Bookheimer, S.Y., Dapretto, M., Deen, B., Delmonte, S., Dinstein, I., Ertl-Wagner, B., Fair, D.A., Gallagher, L., Kennedy, D.P., Keown, C.L., Keysers, C., Lainhart, J.E., Lord, C., Luna, B., Menon, V., Minshew, N.J., Monk, C.S., Mueller, S., Müller, R.-A., Nebel, M.B., Nigg, J.T., O'Hearn, K., Pelphrey, K.A., Peltier, S.J., Rudie, J.D., Sunaert, S., Thioux, M., Tyszka, J.M., Uddin, L.Q., Verhoeven, J.S., Wenderoth, N., Wiggins, J.L., Mostofsky, S.H., Milham, M.P., 2014. The autism brain imaging data exchange: towards a large-scale evaluation of the intrinsic brain architecture in autism. Mol. Psychiatry 19, 659–667. http://dx.doi.org/10.1038/mp.2013.78, (URL ⟨http://www.nature.com/doifinder/10.1038/mp.2013.78⟩).

Fair, D.A., Cohen, A.L., Dosenbach, N.U.F., Church, J.a., Miezin, F.M., Barch, D.M., Raichle, M.E., Petersen, S.E., Schlaggar, B.L., 2008. The maturing architecture of the brain's default network. Proc. Natl. Acad. Sci. U. S. A 105, 4028–4032. http://dx.doi.org/10.1073/pnas.0800376105.

Garrett, D.D., Kovacevic, N., McIntosh, A.R., Grady, C.L., 2011. The importance of being variable. J. Neurosci. 31, 4496–4503. http://dx.doi.org/10.1523/JNEUROSCI.5641-10.2011, (URL ⟨http://www.jneurosci.org/cgi/doi/10.1523/JNEUROSCI.5641-10.2011⟩).

Garrett, D.D., Kovacevic, N., McIntosh, A.R., Grady, C.L., 2013a. The modulation of bold variability between cognitive states varies by age and processing speed. Cereb. Cortex 23, 684–693. http://dx.doi.org/10.1093/cercor/bhs055, (URL ⟨http://www.cercor.oxfordjournals.org/cgi/doi/10.1093/cercor/bhs055⟩).

Garrett, D.D., Samanez-Larkin, G.R., MacDonald, S.W.S., Lindenberger, U., McIntosh, A.R., Grady, C.L., 2013b. Moment-to-moment brain signal variability: a next frontier in human brain mapping? Neurosci. Biobehav. Rev. 37, 610–624. http://dx.doi.org/10.1016/j.neubiorev.2013.02.015, (URL ⟨http://dx.doi.org/10.1016/j.neubiorev.2013.02.015⟩arXiv:NIHMS150003).

Garrett, D.D., McIntosh, A.R., Grady, C.L., 2014. Brain signal variability is parametrically modifiable. Cereb. Cortex 24, 2931–2940. http://dx.doi.org/10.1093/cercor/bht150, (URL ⟨http://www.cercor.oxfordjournals.org/cgi/doi/10.1093/cercor/bht150⟩).

Ghosh, A., Rho, Y., McIntosh, A.R., K??tter, R., Jirsa, V.K., 2008. Noise during rest enables the exploration of the brain's dynamic repertoire. PLoS Comput. Biol. 4. http://dx.doi.org/10.1371/journal.pcbi.1000196.

Gopal, S., Miller, R.L., Michael, A., Adali, T., Cetin, M., Rachakonda, S., Bustillo, J.R., Cahill, N., Baum, S.A., Calhoun, V.D., 2016. Spatial variance in resting fmri networks of schizophrenia patients: an independent vector analysis. Schizophr. Bull. 42, 152–160. http://dx.doi.org/10.1093/schbul/sbv085.

Gothelf, D., Schaer, M., Eliez, S., 2008. Genes, brain development and psychiatric phenotypes in velo-cardio-facial syndrome. Dev. Disabil. Res. Rev. 14, 59–68. http://dx.doi.org/10.1002/ddrr.9.

Grady, C.L., Garrett, D.D., 2014. Understanding variability in the BOLD signal and why it matters for aging. Brain Imaging Behav. 8, 274–283. http://dx.doi.org/10.1007/s11682-013-9253-0, (URL ⟨http://www.pubmedcentral.nih.gov/articlerender.fcgi?artid=3922711&tool=pmcentrez&rendertype=abstract⟩).

Greicius, M.D., Krasnow, B., Reiss, A.L., Menon, V., 2003. Functional connectivity in the resting brain: a network analysis of the default mode hypothesis. Proc. Natl. Acad. Sci. USA 100, 253–258.

Han, Y., Wang, J., Zhao, Z., Min, B., Lu, J., Li, K., He, Y., Jia, J., 2011. Frequency-dependent changes in the amplitude of low-frequency fluctuations in amnestic mild cognitive impairment: a resting-state fMRI study. Neuroimage 55, 287–295. http://dx.doi.org/10.1016/j.neuroimage.2010.11.059, (URL ⟨http://www.dx.doi.org/10.1016/j.neuroimage.2010.11.059⟩).

Hasenkamp, W., James, G.A., Boshoven, W., Duncan, E., 2011. Altered engagement of attention and default networks during target detection in schizophrenia. Schizophr. Res. 125, 169–173. http://dx.doi.org/10.1016/j.schres.2010.08.041.

Jalbrzikowski, M., Jonas, R., Senturk, D., Patel, A., Chow, C., Green, M.F., Bearden, C.E., 2013. Structural abnormalities in cortical volume, thickness, and surface area in 22q11.2 microdeletion syndrome: relationship with psychotic symptoms. NeuroImage Clin. 3, 405–415. http://dx.doi.org/10.1016/j.nicl.2013.09.013, (URL ⟨http://www.dx.doi.org/10.1016/j.nicl.2013.09.013⟩).

Jung, W.H., Jang, J.H., Byun, M.S., An, S.K., Kwon, J.S., 2010. Structural brain alterations in individuals at ultra-high risk for psychosis: a review of magnetic resonance imaging studies and future directions. J. Korean Med. Sci. 25, 1700–1709. http://dx.doi.org/10.3346/jkms.2010.25.12.1700.

Karahanoğlu, F.I., Van De Ville, D., 2015. Transient brain activity disentangles fMRI resting-state dynamics in terms of spatially and temporally overlapping networks. Nat. Commun. 6, 7751. http://dx.doi.org/10.1038/ncomms8751, (URL ⟨http://www.nature.com/doifinder/10.1038/ncomms8751⟩).

Karlsgodt, K.H., van Erp, T.G.M., Bearden, C.E., Cannon, T.D., 2014. Altered relationships between age and functional brain activation in adolescents at clinical

high risk for psychosis. Psychiatry Res. Neuroimaging 221, 21–29. http://dx.doi.org/10.1016/j.pscychresns.2013.08.004, (URL ⟨http://dx.doi.org/10.1016/j.pscychresns.2013.08.004⟩arXiv:NIHMS150003).
Krishnan, A., Williams, L.J., McIntosh, A.R., Abdi, H., 2011. Partial Least Squares (PLS) methods for neuroimaging: a tutorial and review. Neuroimage 56, 455–475. http://dx.doi.org/10.1016/j.neuroimage.2010.07.034.
Lai, M.C., Lombardo, M.V., Chakrabarti, B., Sadek, S.A., Pasco, G., Wheelwright, S.J., Bullmore, E.T., Baron-Cohen, S., Suckling, J., 2010. A shift to randomness of brain oscillations in people with autism. Biol. Psychiatry 68, 1092–1099. http://dx.doi.org/10.1016/j.biopsych.2010.06.027, (URL ⟨http://www.dx.doi.org/10.1016/j.biopsych.2010.06.027⟩).
Laumann, T.O., Gordon, E.M., Adeyemo, B., Snyder, A.Z., un Joo, S.J., Chen, M.Y., Gilmore, A.W., McDermott, K.B., Nelson, S.M., Dosenbach, N.U.F., Schlaggar, B.L., Mumford, J.A., Poldrack, R.A., Petersen, S.E., 2015. Functional system and areal organization of a highly sampled individual human brain. Neuron 87, 657–670. http://dx.doi.org/10.1016/j.neuron.2015.06.037, (URL ⟨http://www.dx.doi.org/10.1016/j.neuron.2015.06.037⟩).
Lewandowski, K.E., Shashi, V., Berry, P.M., Kwapil, T.R., 2007. Schizophrenic-like neurocognitive deficits in children and adolescents with 22q11 deletion syndrome. Am. J. Med. Genet. Part B Neuropsychiatr. Genet 144, 27–36. http://dx.doi.org/10.1002/ajmg.b.30379.
Lippé, S., Kovacevic, N., McIntosh, A.R., 2009. Differential maturation of brain signal complexity in the human auditory and visual system. Front. Hum. Neurosci. 3, 48. http://dx.doi.org/10.3389/neuro.09.048.2009.
Liu, X., Wang, S., Zhang, X., Wang, Z., Tian, X., He, Y., 2014. Abnormal amplitude of low-frequency fluctuations of intrinsic brain activity in Alzheimer's disease. J. Alzheimer'S. Dis. 40, 387–397. http://dx.doi.org/10.3233/JAD-131322.
Liu, C., Xue, Z., Palaniyappan, L., Zhou, L., Liu, H., Qi, C., Wu, G., Mwansisya, T.E., Tao, H., Chen, X., Huang, X., Liu, Z., Pu, W., 2016. Abnormally increased and incoherent resting-state activity is shared between patients with schizophrenia and their unaffected siblings. Schizophr. Res.. http://dx.doi.org/10.1016/j.schres.2016.01.022, (URL ⟨http://linkinghub.elsevier.com/retrieve/pii/S0920996416300214⟩).
Maeder, J., Schneider, M., Bostelmann, M., Debbané, M., Glaser, B., Menghetti, S., Schaer, M., Eliez, S., 2016. Developmental trajectories of executive functions in 22q11.2 deletion syndrome. J. Neurodev. Disord. 8, 10. http://dx.doi.org/10.1186/s11689-016-9141-1, (URL ⟨http://www.jneurodevdisorders.com/content/8/1/10⟩).
Mattiaccio, L.M., Coman, I.L., Schreiner, M.J., Antshel, K.M., Fremont, W.P., Bearden, C.E., Kates, W.R., 2016. Atypical functional connectivity in resting-state networks of individuals with 22q11.2 deletion syndrome: associations with neurocognitive and psychiatric functioning. J. Neurodev. Disord. 8, 2. http://dx.doi.org/10.1186/s11689-016-9135-z, (URL ⟨http://www.jneurodevdisorders.com/content/8/1/2⟩).
McIntosh, A.R., Lobaugh, N.J., 2004. Partial least squares analysis of neuroimaging data: Applications and advances. Neuroimage 23, 250–263. http://dx.doi.org/10.1016/j.neuroimage.2004.07.020.
McIntosh, A., Chau, W., Protzner, A., 2004. Spatiotemporal analysis of event-related fMRI data using partial least squares. Neuroimage 23, 764–775. http://dx.doi.org/10.1016/j.neuroimage.2004.05.018, (URL ⟨http://linkinghub.elsevier.com/retrieve/pii/S1053811904002976⟩).
McIntosh, A.R., Kovacevic, N., Itier, R.J., 2008. Increased brain signal variability accompanies lower behavioral variability in development. PLoS Comput. Biol., 4. http://dx.doi.org/10.1371/journal.pcbi.1000106.
McIntosh, A.R., Kovacevic, N., Lippe, S., Garrett, D., Grady, C., Jirsa, V., 2010. The development of a noisy brain. Arch. Ital. Biol. 148, 323–337. http://dx.doi.org/10.4449/aib.v148i3.1225.
Menon, V., Uddin, L.Q., 2010. Saliency, switching, attention and control: a network model of insula function. Brain Struct. Funct., 1–13. http://dx.doi.org/10.1007/s00429-010-0262-0.
Menon, V., 2011. Large-scale brain networks and psychopathology: a unifying triple network model. Trends Cogn. Sci. 15, 483–506. http://dx.doi.org/10.1016/j.tics.2011.08.003, (URL ⟨http://www.dx.doi.org/10.1016/j.tics.2011.08.003⟩).
Misić, B., Mills, T., Taylor, M.J., McIntosh, A.R., 2010. Brain noise is task dependent and region specific. J. Neurophysiol. 104, 2667–2676. http://dx.doi.org/10.1152/jn.00648.2010.
Murphy, K., Jones, L., Owen, M., 1999. High rates of schizophrenia in adults with velo-cardio-facial syndrome. Arch. Gen. Psychiatry 56, 940–945. http://dx.doi.org/10.1001/archpsyc.56.10.940, (URL +⟨http://www.dx.doi.org/10.1001/archpsyc.56.10.940⟩).
Niklasson, L., Gillberg, C., 2010. The neuropsychology of 22q11 deletion syndrome. A neuropsychiatric study of 100 individuals. Res. Dev. Disabil. 31, 185–194. http://dx.doi.org/10.1016/j.ridd.2009.09.001.
Oskarsdóttir, S., Vujic, M., Fasth, A., 2004. Incidence and prevalence of the 22q11 deletion syndrome: a population-based study in western sweden. Arch. Dis. Child. 89, 148–151. http://dx.doi.org/10.1136/adc.2003.026880.
Padula, M.C., Schaer, M., Scariati, E., Schneider, M., Van De Ville, D., Debbané, M., Eliez, S., 2015. Structural and functional connectivity in the default mode network in 22q11.2 deletion syndrome. J Neurodev. Disord. 7, 23. http://dx.doi.org/10.1186/s11689-015-9120-y, (URL ⟨http://www.jneurodevdisorders.com/content/7/1/23⟩).
Pankow, A., Deserno, L., Walter, M., Fydrich, T., Bermpohl, F., Schlagenhauf, F., Heinz, A., 2015. Reduced default mode network connectivity in schizophrenia patients. Schizophr. Res. 165, 90–93. http://dx.doi.org/10.1016/j.schres.2015.03.027, (URL ⟨http://www.dx.doi.org/10.1016/j.schres.2015.03.027⟩).
Poldrack, R.A., Laumann, T.O., Koyejo, O., Gregory, B., Hover, A., Chen, M.-Y., Gorgolewski, K.J., Luci, J., Joo, S.J., Boyd, R.L., Hunicke-Smith, S., Simpson, Z.B., Caven, T., Sochat, V., Shine, J.M., Gordon, E., Snyder, A.Z., Adeyemo, B., Petersen, S.E., Glahn, D.C., Reese Mckay, D., Curran, J.E., Göring, H.H.H., Carless, M.A., Blangero, J., Dougherty, R., Leemans, A., Handwerker, D.A., Frick, L., Marcotte, E.M., Mumford, J.A., 2015. Long-term neural and physiological phenotyping of a single human. Nat. Commun. 6, 8885. http://dx.doi.org/10.1038/ncomms9885, (URL ⟨http://www.nature.com/ncomms/2015/151209/ncomms9885/full/ncomms9885.html⟩).
Power, J.D., Barnes, K.a., Snyder, A.Z., Schlaggar, B.L., Petersen, S.E., 2012. Spurious but systematic correlations in functional connectivity MRI networks arise from subject motion. Neuroimage 59, 2142–2154. http://dx.doi.org/10.1016/j.neuroimage.2011.10.018, (URL ⟨http://www.dx.doi.org/10.1016/j.neuroimage.2011.10.018⟩arXiv:NIHMS150003).
Power, J.D., Mitra, A., Laumann, T.O., Snyder, A.Z., Schlaggar, B.L., Petersen, S.E., 2014. Methods to detect, characterize, and remove motion artifact in resting state fMRI. Neuroimage 84, 320–341. http://dx.doi.org/10.1016/j.neuroimage.2013.08.048, (URL http://www.dx.doi.org/10.1016/j.neuroimage.2013.08.048⟩arXiv:NIHMS150003).
Qin, P., Northoff, G., 2011. How is our self related to midline regions and the default-mode network? Neuroimage 57, 1221–1233. http://dx.doi.org/10.1016/j.neuroimage.2011.05.028, (URL ⟨http://www.dx.doi.org/10.1016/j.neuroimage.2011.05.028⟩).
Richiardi, J., Gschwind, M., Simioni, S., Annoni, J.-M., Greco, B., Hagmann, P., Schluep, M., Vuilleumier, P., Van De Ville, D., 2012. Classifying minimally disabled multiple sclerosis patients from resting state functional connectivity. Neuroimage 62, 2021–2033. http://dx.doi.org/10.1016/j.neuroimage.2012.05.078, (URL ⟨http://linkinghub.elsevier.com/retrieve/pii/S1053811912005666⟩).
Scariati, E., Schaer, M., Richiardi, J., Schneider, M., Debbané, M., Van De Ville, D., Eliez, S., 2014. Identifying 22q11.2 deletion syndrome and psychosis using resting-state connectivity patterns. Brain Topogr. 27, 808–821. http://dx.doi.org/10.1007/s10548-014-0356-8, (URL ⟨http://link.springer.com/10.1007/s10548-014-0356-8⟩).
Schaer, M., Debbané, M., Bach Cuadra, M., Ottet, M.-C., Glaser, B., Thiran, J.-P., Eliez, S., 2009. Deviant trajectories of cortical maturation in 22q11.2 deletion syndrome (22q11DS): a cross-sectional and longitudinal study. Schizophr. Res 115, 182–190. http://dx.doi.org/10.1016/j.schres.2009.09.016, (URL ⟨http://linkinghub.elsevier.com/retrieve/pii/S0920996409004356⟩).
Schmitt, J.E., Vandekar, S., Yi, J., Calkins, M.E., Ruparel, K., Roalf, D.R., Whinna, D., Souders, M.C., Satterwaite, T.D., Prabhakaran, K., McDonald-McGinn, D.M., Zackai, E.H., Gur, R.C., Emanuel, B.S., Gur, R.E., 2015. Aberrant cortical morphometry in the 22q11.2 deletion syndrome. Biol. Psychiatry 78, 135–143. http://dx.doi.org/10.1016/j.biopsych.2014.10.025, (URL ⟨http://www.sciencedirect.com/science/article/pii/S0006322314008907⟩).
Schneider, M., Schaer, M., Mutlu, A.K., Menghetti, S., Glaser, B., Debbané, M., Eliez, S., 2014. Clinical and cognitive risk factors for psychotic symptoms in 22q11.2 deletion syndrome: a transversal and longitudinal approach. Eur. Child Adolesc. Psychiatry 23, 425–436. http://dx.doi.org/10.1007/s00787-013-0469-8.
Schreiner, M.J., Karlsgodt, K.H., Uddin, L.Q., Chow, C., Congdon, E., Jalbrzikowski, M., Bearden, C.E., 2014. Default mode network connectivity and reciprocal social behavior in 22q11.2 deletion syndrome. Soc. Cogn. Affect. Neurosci. 9, 1261–1267. http://dx.doi.org/10.1093/scan/nst114.
Shashi, V., Veerapandiyan, A., Keshavan, M.S., Zapadka, M., Schoch, K., Kwapil, T.R., Hooper, S.R., Stanley, J.A., 2012. Altered development of the dorsolateral prefrontal cortex in chromosome 22q11.2 deletion syndrome: an in vivo proton spectroscopy study. Biol. Psychiatry 72, 684–691. http://dx.doi.org/10.1016/j.biopsych.2012.04.023.
Sherman, L.E., Rudie, J.D., Pfeifer, J.H., Masten, C.L., McNealy, K., Dapretto, M., 2014. Development of the Default Mode and Central Executive Networks across early adolescence: a longitudinal study. Dev. Cogn. Neurosci. 10, 148–159. http://dx.doi.org/10.1016/j.dcn.2014.08.002, (URL ⟨http://www.dx.doi.org/10.1016/j.dcn.2014.08.002⟩).
Spreng, R.N., Mar, R.A., Kim, A.S.N., 2008. The common neural basis of autobiographical memory, prospection, navigation. Theory Mind, Default Mode: A Quant. Meta-Anal. J. Cogn. Neurosci. 21, 489–510. http://dx.doi.org/10.1162/jocn.2008.21029, (URL ⟨http://dx.doi.org/10.1162/jocn.2008.21029$\delimiter"026E30F$n ⟨http://www.mitpressjournals.org/doi/abs/10.1162/jocn.2008.21029?url_ver=Z39.88-2003 & rfr_id=ori:rid:crossref.org & rfr_dat=cr_pub=pubmed$\delimiter"026E30F$n ⟨http://www.mitpressjournals.org/doi/pdf/10.1162/jocn.2008.21029?url_ver=Z39.8).
Sun, D., Phillips, L., Velakoulis, D., Yung, A., McGorry, P.D., Wood, S.J., van Erp, T.G.M., Thompson, P.M., Toga, A.W., Cannon, T.D., Pantelis, C., 2009. Progressive brain structural changes mapped as psychosis develops in 'at risk' individuals. Schizophr. Res. 108, 85–92. http://dx.doi.org/10.1016/j.schres.2008.11.026, (URL ⟨http://dx.doi.org/10.1016/j.schres.2008.11.026⟩).
Supekar, K., Uddin, L.Q., Prater, K., Amin, H., Greicius, M.D., Menon, V., 2010. Development of functional and structural connectivity within the default mode network in young children. Neuroimage 52, 290–301. http://dx.doi.org/10.1016/j.neuroimage.2010.04.009, (URL ⟨http://www.dx.doi.org/10.1016/j.neuroimage.2010.04.009⟩).
Swillen, A., Devriendt, K., Legius, E., Eyskens, B., Dumoulin, M., Gewillig, M., Fryns, J.P., 1997. Intelligence and psychosocial adjustment in velocardiofacial syndrome: a stidy of 37 children and adolescnets with VCFS. J. Med. Genet. 34, 453–458, (URL ⟨http://www.scopus.com/inward/record.url?eid=2-s2.0-33748137328 & partnerID=40 & md5=e1f6e3f243a79525f3f680f848cab88f⟩).
van den Heuvel, M.P., Sporns, O., 2013. Network hubs in the human brain. Trends Cogn. Sci. 17, 683–696. http://dx.doi.org/10.1016/j.tics.2013.09.012.
Wechsler, D., 1991. Weschler intelligence scale for children. San. Antonio TX Psychol. Corp..
Wechsler, D., 1997. Wechsler intelligence scale for adults. Lond. Psychol. Corp..

Wu, C.W., Chen, C.-L., Liu, P.-Y., Chao, Y.-P., Biswal, B.B., Lin, C.-P., 2011. Empirical Evaluations of Slice-Timing, Smoothing, and Normalization Effects in Seed-Based, Resting-State Functional Magnetic Resonance Imaging Analyses. Brain Connect 1, 401–410. http://dx.doi.org/10.1089/brain.2011.0018.

Xi, Q., Zhao, X., Wang, P., Guo, Q., Jiang, H., Cao, X., He, Y., Yan, C., 2012. Spontaneous brain activity in mild cognitive impairment revealed by amplitude of low-frequency fluctuation analysis: a resting-state fMRI study. Radiol. Medica 117, 865–871. http://dx.doi.org/10.1007/s11547-011-0780-8.

Yan, 2010. DPARSF: a MATLAB toolbox for "pipeline" data analysis of resting-state fMRI. Front. Syst. Neurosci., 4, 1–7. http://dx.doi.org/10.3389/fnsys.2010.00013.

Yang, G.J., Murray, J.D., Repovs, G., Cole, M.W., Savic, A., Glasser, M.F., Pittenger, C., Krystal, J.H., Wang, X.-J., Pearlson, G.D., Glahn, D.C., Anticevic, A., 2014. Altered global brain signal in schizophrenia. Proc. Natl. Acad. Sci. 111, 7438–7443. http://dx.doi.org/10.1073/pnas.1405289111, (URL ⟨http://www.pnas.org/cgi/doi/10.1073/pnas.1405289111⟩).

Yu, R., Chien, Y.L., Wang, H.L.S., Liu, C.M., Liu, C.C., Hwang, T.J., Hsieh, M.H., Hwu, H.G., Tseng, W.Y.I., 2014. Frequency-specific alternations in the amplitude of low-frequency fluctuations in schizophrenia. Hum. Brain Mapp. 35, 627–637. http://dx.doi.org/10.1002/hbm.22203.

Zalesky, A., Fornito, A., Bullmore, E., 2012. On the use of correlation as a measure of network connectivity. Neuroimage 60, 2096–2106. http://dx.doi.org/10.1016/j.neuroimage.2012.02.001.

Zang, Y., He, Y., Zhu, C., Cao, Q., Sui, M., Liang, M., Tian, L., Jiang, T., Wang, Y., 2007. Altered baseline brain activity in children with ADHD revealed by resting-state functional MRI. Brain Dev. 29, 83–91. http://dx.doi.org/10.1016/j.braindev.2006.07.002, (URL ⟨http://www.ncbi.nlm.nih.gov/entrez/query.fcgi?db=pubmed&cmd=Retrieve&dopt=AbstractPlus&list_uids=16919409/papers2://publication/uuid/3C9F76F1-C1FB-4B43-8CF5-51815A9397A2⟩).

Zapala, M., Schork, N., 2006. Multivariate regression analysis of distance matrices for testing associations between gene expression patterns and related variables. Proc. Natl. Acad. Sci. 103, (URL ⟨http://www.pnas.org/content/103/51/19430.full⟩).

Zhao, Z.-L., Fan, F.-M., Lu, J., Li, H.-J., Jia, L.-F., Han, Y., Li, K.-C., 2014. Changes of gray matter volume and amplitude of low-frequency oscillations in amnestic {MCI:} an integrative multi-modal {MRI} study. Acta Radiol. 56, 614–621. http://dx.doi.org/10.1177/0284185114533329, (URL ⟨http://www.dx.doi.org/10.1177/0284185114533329⟩).